CHAPTER III

Results

3.1 Changes of the midgut from female *An. dissidens* during adult development and after blood feeding

3.1.1 Midgut Morphology

Light microscopy revealed that the midgut epithelium was a single layer of polarized cells. On one side, the midgut cells were bound to a basement membrane, which faced the body cavity and hemolymph of the mosquito, and on the other, the apical cell surfaces faced the midgut lumen. Transmission electron microscopy (TEM) showed that the midgut epithelium comprised a monolayer of columnar polarized cells, which lay on a non-cellular basal lamina (Figure 3.1). Many mitochondria, cisterns of rough endoplasmic reticulum (RER), a smooth endoplasmic reticulum (SER), nucleus, free ribosome and vesicle with electron-lucent content (EDV) were observed in the apical cytoplasm. Apical membranes formed microvilli that protruded into the midgut lumen. Also, the vesicle with electron-lucent content moved toward the apical membrane, where the content was released into the midgut.

The sugar fed midgut of female *An. dissidens* was observed during adult development under scanning electron microscopy (SEM), and examined on different days post emergence, i.e. early emergence, and day 1, 3, 5, 8, 10, 16 and 21. Yellow bodies (YBs) were found in the midgut lumen, covering the microvilli surfaces at the beginning of adult emergence (Figure 3.2a). However, no YBs being seen after the first day of emergence. The microvilli-covered apical cell surfaces were well-developed, as shown in Figure 3.2b, where individual mounds with cell junctions recessed from the cell center. Enlarged apical protrusions in the midgut lumen (Figure 3.2b) were observed occasionally. A large number of cells appeared clearly at 3 days post emergence, and the microvilli-covered apical cell surfaces were exposed indirectly to the lumen (Figure 3.2c).

The microvilli were covered by a network of branching fibers that are called the microvilli-associated network (MN), as shown in Figure 3.2c and d. However, changes in the midgut structure, caused by the aging process, were not significantly different to the various times shown in Figure 3.2.

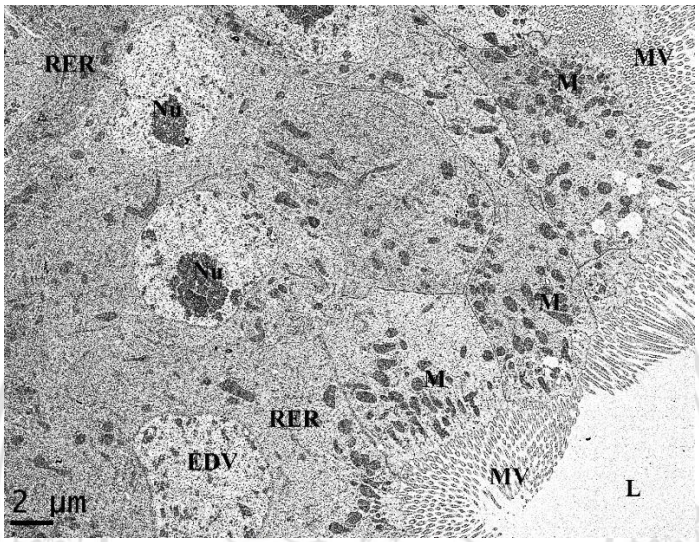

Figure 3.1 TEM micrograph of midgut epithelial cells of the *An. dissidens* mosquito. The epithelial cell is formed by a single layer of columnar cells. TEM image showing that the apical surface has a long microvilli (MV) that protrudes into the midgut lumen (L). Large nucleus (Nu), abundant mitrochondria (M) and rough endoplasmic reticulum (RER) are visualized in the center and apical region of the cell. The vesicle with electron-lucent content (EDV) is distributed in the apical region.

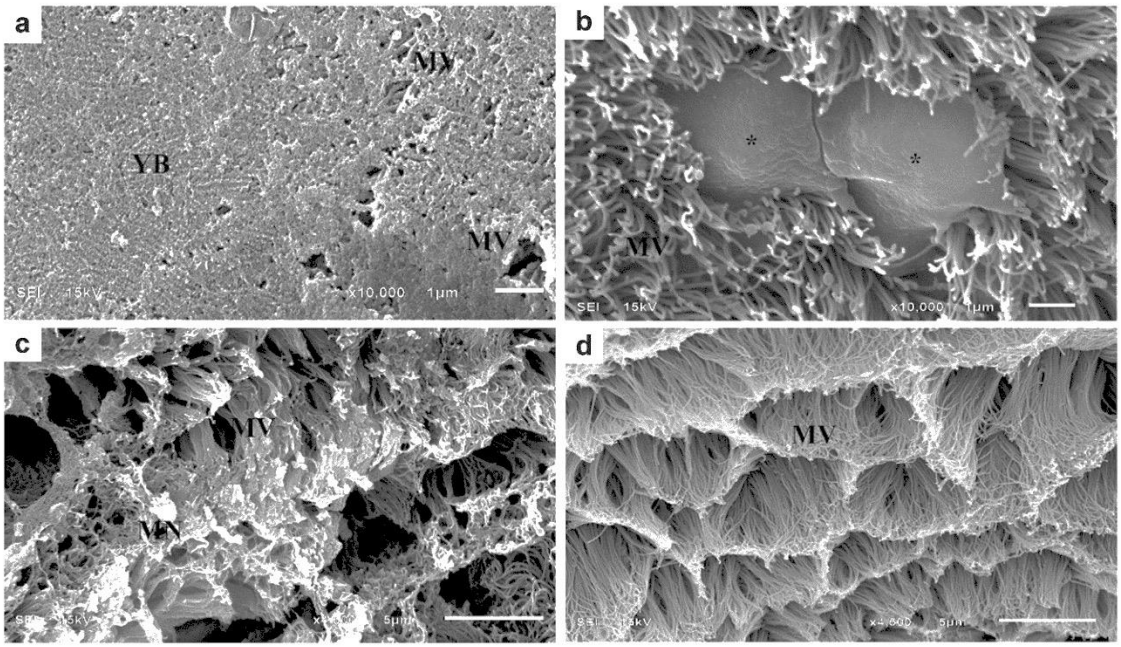

Figure 3.2 SEM micrographs showing changes in the midgut of the *An. dissidens* mosquito during development. a-d) The microvilli (MV), yellow body (YB), and microvilli-associated network (MN) are visualized on the lumen side of the mosquito midgut. a) At the newly emerged stage, the microvilli-covered apical cell surfaces are covered by a yellow body (YB). The MV appeared through some holes of the YB. b) The midguts cleaned from the YB show bare cells (*) on the midgut surface at 1 day old. c) The MN is above the MV at 3 days old as well as (d) on the lumen side of the midgut at 21 days old.

The midguts of blood-fed female mosquitoes were observed under SEM and examined at different time points (0, 3, 6, 12, 24 and 72 h after blood feeding). Immediately the mosquito became engorged, the midgut epithelium expanded greatly, and the midgut did not protrude from the microvilli (Figure 3.3a). The epithelial cells of the midgut were flattened with short brush border microvilli 3 h after blood feeding. Meanwhile, the initial formation of the PM was found close to the apical cell surfaces (Figure 3.3b). This PM formation revealed numerous granular materials surrounding the apical cell surface, and most of them became compacted. The PM formation reached completion within 6 h after blood feeding, with a thicker layer than that after 3 h blood feeding (Figure 3.3c). The midgut began its last phase of PM formation 12 h after blood feeding, as the PM presented two layers (one electrondense adosed to MV and heme electronlucent above MV) (Figure 3.3d), which were separated by a thin layer. The epithelial cells started to recover their structure from 12 to 24 h after blood feeding (Figure 3.3d-e). Blood digestion ended around 72 h after blood feeding. The epithelial cells returned to the structure observed before blood feeding, and the MN appeared again on the microvilli-covered apical cell surface (Figure 3.3f).

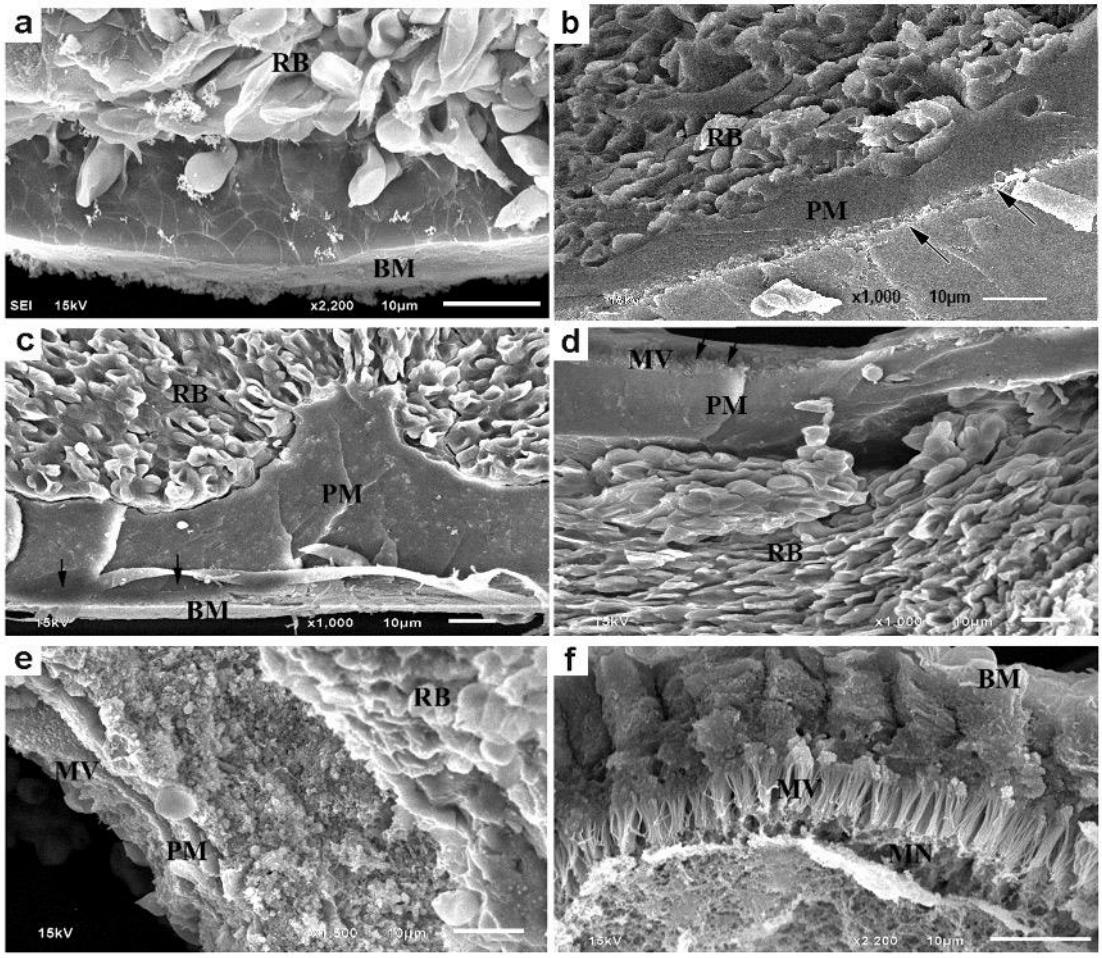

Figure 3.3 SEM micrographs of PM formation in the *An. dissidens* midgut after blood feeding. a) The midgut lumen full of blood meal (RB) and the tiny basal membrane (BM) 1 h after blood feeding. b) The midgut presenting early PM formation within 3 h after blood feeding. The PM between the RB and midgut epithelium (arrow). c) The PM being well enveloped together with the midgut lumen 6 h after blood feeding, and the PM being thicker than that 3 h after blood feeding. d and e) The late phase of blood digestion starting from 12 to 24 h after blood feeding, as the fractured midgut is separated by the midgut epithelium (arrow), PM, and RB. f) The midgut morphology returns to the same state as that before blood feeding. The microvilli-associated network (MN) is above the microvilli (MV).

3.1.2 Analysis of midgut proteins of female *An. dissidens*

The midgut proteins of sugar-fed *An. dissidens* were analyzed by 2-DE in a non-linear gradient pI 3-10 (Figure 3.4). Approximately 150 protein spots were detected from the mosquitoes on 3-5 days old and distributed in the range of a molecular mass between 10 and 116 kDa and, the range of pI between 4.7 and 9.5. Sixty-six protein spots were selected to identify by nanoLC-MS and assigned with Mascot search engine using the mosquito vector database. Identified proteins were summarized in Table 3.1.

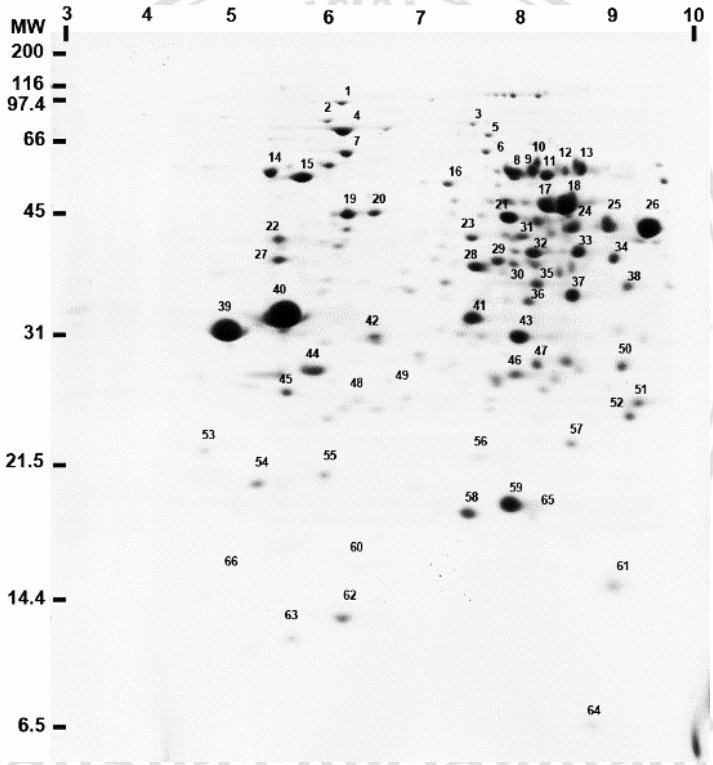

Figure 3.4 2-DE analysis of the female midguts from the sugar fed *An. dissidens* on 3-5 days old. Proteins were separated in the first dimension across a non-linear pH range of 3-10 NL, and in the second dimension in a 15% SDS-PAGE. The gels were stained with Coomassie blue. Molecular mass markers are indicated on the left in kDa. Isoelectric points (pI) are indicated at the top.

Table 3.1 Midgut proteins of female *An. dissidens* identified by nanoLC-MS.

SN[a]	Exp. (MW[d]/pI[e])		NCBI accesion NO.[b]	Protein score[c]	Theo. (MW[d]/pI[e])		Matching peptide	% coverage	Protein sequences			Recommended name	Biological process catergories
1	100	6.1	XP_001662523.1	425	80.29	5.44	10(4)	15%	K	EMVELPLR	H	Spermatogenesis associated factor	Unknown metabolic process
									K	LAGESESNLR	K		
									R	GGNVGDAGGAADR	V		
									R	GILMYGPPGTGK	T		
									R	GVLFYGPPGCGK	T		
									R	EIDIGIPDATGR	L		
									K	AIANECQANFISVK	G		
									K	AIANECQANFISVK	G		
									K	VTQGFSGADLTEICQR	A		
									R	ELQELVQYPVEHPDK	F		
2	85	5.9	XP_313085.3	620	72.81	5.15	16(5)	18%	R	LTPDDIER	M	Heat shock 70kDa protein 5	Protein folding
									K	IVITNDQNR	L		
									K	IVITNDQNR	L		
									K	FDLTGIPPAPR	G		
									K	FDLTGIPPAPR	G		
									K	FDLTGIPPAPR	G		
									R	NELESYAYSLK	N		
									R	NELESYAYSLK	N		
									K	FEELNMDLFR	S		
									K	ELEDIVQPIIAK	L		
									K	ELEDIVQPIIAK	L		
									R	ITPSYVAFTADGER	L		
									R	IINEPTAAAIAYGLDK	K		
									K	NQLTTNPENTVFDAK	R		
									R	IINEPTAAAIAYGLDKK	D		
									K	VTHAVVTVPAYFNDAQR	Q		
3	80	7.7	XP_321442.4	274	80	6.43	8(3)	8%	R	LIAPMLR	N	NADH dehydrogenase (ubiquinone) Fe-S protein 1	ATP biosynthetic process
									R	MCLVEVEK	S		
									R	YEAPLLNTR	L		
									R	YEAPLLNTR	L		
									K	QGTYVNTEGR	A		
									K	LADFFMTDPITR	A		

Table 3.1 (continued)

SN[a]	Exp. (MW[d]/pI[e])		NCBI accession NO.[b]	Protein score[c]	Theo. (MW[d]/pI[e])		Matching peptide	% coverage	Protein sequences			Recommended name	Biological process categories
4	70	6.1	XP_001689308.2	766	71.67	5.32	18(7)	20%	R	LSKEDIER	M	Heat shock 70kDa protein 1/8	Protein folding
									R	LSKEDIER	M		
									K	LLQDFFNGK	E		
									K	LLQDFFNGK	E		
									K	FELSGIPPAPR	G		
									K	FELSGIPPAPR	G		
									K	FELSGIPPAPR	G		
									K	DAGTISGLNVLR	I		
									K	DAGTISGLNVLR	I		
									K	VEIIANDQGNR	T		
									K	VEIIANDQGNR	T		
									R	LVNHFAQEFK	R		
									R	FEELNADLFR	S		
									K	ASIHDIVLVGGSTR	I		
									R	ARFEELNADLFR	S		
									R	TTPSYVAFTDTER	L		
									K	TVTNAVITVPAYFNDSQR	Q		
5	65	7.9	XP_001863331.1	242	66.51	6.23	7(2)	10%	K	FIYATLPR	T	wd-repeat protein	rRNA processing
									K	DITVLKDNR	K		
									R	GQPIVLGGDPK	G		
									K	DISWSPDSQR	I		
									K	NEFQPIGGPIK	D		
									K	YSPSGFYIASGDQSGK	I		
									K	YSPSGFYIASGDQSGK	I		
6	60	7.6	XP_313043.5	335	63.89	6.05	11(1)	13%	K	FGLIYR	R	Malate dehydrogenase (oxaloacetate-decarboxylating)(NADP+)	Carbohydrate metabolism
									R	YQEDLNK	Y		
									R	GHVFDVLR	N		
									R	NWPEPDVR	A		
									K	GLAFTLEER	Q		
									K	GLAFTLEER	Q		
									K	GLAFTLEER	Q		
									R	GLFVTINDR	G		

Table 3.1 (continued)

SN[a]	Exp. (MW[d]/pI[e])		NCBI accession NO.[b]	Protein score[c]	Theo. (MW[d]/pI[e])		Matching peptide	% coverage	Protein sequences			Recommended name	Biological process categories
									R	QILGIHGLQPAR	F		
7	60	6.2	XP_318461.2	838	61.03	5.55	23(13)	29%	K	APGFGDNR	K	60 coda heat shock protein, mitochondrial precursor	Protein folding
									K	IGLQVAAVK	A		
									K	IGLQVAAVK	A		
									R	CAPALANLK	G		
									R	VNDALCATR	A		
									R	VNDALCATR	A		
									R	VNDALCATR	A		
									K	NAGVDGSVVVAK	V		
									K	NAGVDGSVVVAK	V		
									K	NAGVDGSVVVAK	V		
									R	AIGDLISEAMK	R		
									R	AIGDLISEAMK	R		
									K	VGGSSEVEVNEK	K		
									R	AIGDLISEAMKR	V		
									R	NVILEQSWGSPK	I		
									R	NVILEQSWGSPK	I		
									K	VGGSSEVEVNEKK	D		
									R	GYISPYFINSSK	G		
									K	TLNDELEVIEGMK	F		
									R	AAVEEGIVPGGGTALIR	C		
									R	AAVEEGIVPGGGTALIR	C		
									K	TLNDELEVIEGMKFDR	G		
									K	ISTVQSIIPALEMANQQR	K		
									R	KVNTPEEIAQVATISANG	A		
									R	KVNTPEEIAQVATISANG	A		
8	56	7.95	ETN60725.1	426	54.00	6.44	8(6)	16%	K	FPFAANSR	A	Dihydrolipoamide dehydrogenase	Cell redox homeostasis
									K	FPFAANSR	A		
									K	TNNDTDGFVK	V		
									R	RPYTEGLGLENVGIVK	D		
									R	RPYTEGLGLENVGIVK	D		
									K	NEEELKAEGVAYNVGK	F		

Table 3.1 (continued)

SN[a]	Exp. (MW[d]/pI[e])		NCBI accession NO.[b]	Protein score[c]	Theo. (MW[d]/pI[e])		Matching peptide	% coverage	Protein sequences			Recommended name	Biological process categories
9													
10	58	8.2	XP_001652343.1	297	54.14	6.36	5(3)	12%	K	TNNDTDGFVK	V	Dihydrolipoamide dehydrogenase	Cell redox homeostasis
									R	RPYTEGLGLENVGIVK	D		
									R	RPYTEGLGLENVGIVK	D		
									K	NDTLGGTCLNVGCIPSK	A		
11	55	8.3	XP_313425.3	516	56.90	8.07	15(5)	20%	R	TTLELGGK	S	Aldehyde dehydrogenase (NAD+)	Cell redox homeostasis
									K	ILGLIDTGK	Q		
									K	SLDEVIER	A		
									K	IYDEFVER	S		
									K	VIAEIQQGTK	A		
									K	ADIDQAVVAAR	D		
									K	ADIDQAVVAAR	D		
									K	IQQGSGLSNLK	R		
									K	IQQGSGLSNLK	R		
									K	IQQGSGLSNLK	R		
									K	IQQGSGLSNLK	R		
									K	SPNIILSDADMK	H		
									K	VIPMDGEFFVYTR	H		
									K	VIPMDGEFFVYTR	H		
									R	TVGNPFDLTTEHGPQVDR	A		
12	56	8.6	XP_001845679.1	178	51.49	9.23	5(2)	8%	K	GLVVPVLR	N	Dihydrolipoamide succinyltransferase component of 2-oxoglutarate dehydrogenase	Carbohydrate metabolic process
									K	VPPADYSK	E		
									R	HAQAIEAATVK	V		
									R	HAQAIEAATVK	V		
									K	VPPFADSVSEGDVK	F		
13	57	8.89	XP_315228.5	416	56.80	7.56	11(5)	19%	R	CPIIAVTR	F	Pyruvate kinase	Carbohydrate metabolic process
									R	VQYGIEFGK	E		
									K	QGSGFTNTIR	V		
									K	QGSGFTNTIR	V		
									R	GDLGIEIPAEK	V		
									R	AAAIIVITTSGR	S		
									K	IYVDYVNIVK	V		

Table 3.1 (continued)

SN[a]	Exp. (MW[d]/pI[e])		NCBI accession NO.[b]	Protein score[c]	Theo. (MW[d]/pI[e])		Matching peptide	% coverage	Protein sequences			Recommended name	Biological process categories
									K	GEYPLECVLTMAK	T		
									R	GFLKPGNPIVVVTGWK	Q		
14	54	5.48	ABF18266.1	558	53.94	5.03	14(8)	20%	R	VLDTGSPIR	I	F0F1-type ATP synthase beta subunit	ATP biosynthetic process
									R	VLDTGSPIR	I		
									K	IGLFGGAGVGK	T		
									K	IGLFGGAGVGK	T		
									K	LVPLEETIK	G		
									R	IINVIGEPIDER	G		
									R	IINVIGEPIDER	G		
									R	FTQAGSEVSALLGR	I		
									R	FTQAGSEVSALLGR	I		
									R	VALTGLTVAEYFR	D		
									K	TVLIMELINNVAK	A		
15	49	5.8	ETN62038.1	1317	53.73	5.02	38(25)	45%	R	VLDTGSPIR	I	ATP synthase beta subunit	ATP biosynthetic process
									R	IMDPNIIGAEHYNIAR	G		
									R	VLDTGSPIR	I		
									R	VLDTGSPIR	I		
									K	IGLFGGAGVGK	T		
									K	IGLFGGAGVGK	T		
									K	IGLFGGAGVGK	T		
									K	IGLFGGAGVGK	T		
									R	IPVGAETLGR	I		
									R	IPVGAETLGR	I		
									K	LVPLEETIK	G		
									K	LVPLEETIK	G		
									K	LVPLEETIK	G		
									K	VVDLLAPYAK	G		
									K	VVDLLAPYAK	G		
									K	VVDLLAPYAK	G		
									K	VVDLLAPYAK	G		
									R	TIAMDGTEGLVR	G		
									R	IINVIGEPIDER	G		

Table 3.1 (continued)

SN[a]	Exp. (MW[d]/pI[e])		NCBI accession NO.[b]	Protein score[c]	Theo. (MW[d]/pI[e])		Matching peptide	% coverage	Protein sequences			Recommended name	Biological process categories
15	49	5.8	ETN62038.1	1317	53.73	5.02	38(25)	45%	K	AHGGYSVFAGVGER	T	ATP synthase beta subunit	ATP biosynthetic process
									R	FTQAGSEVSALLGR	I		
									R	FTQAGSEVSALLGR	I		
									R	FTQAGSEVSALLGR	I		
									R	VALTGLTVAEYFR	D		
									K	AHGGYSVFAGVGER	T		
									R	VALTGLTVAEYFR	D		
									K	TVLIMELINNVAK	A		
									K	TVLIMELINNVAK	A		
									K	TVLIMELINNVAK	A		
									K	VALVYGQMNEPPGAR	A		
									R	LVLEVAQHLGENTVR	T		
									R	FLSQPFQVAEVFTGHAGK	L		
									R	FLSQPFQVAEVFTGHAGK	L		
									R	AIAELGIYPAVDPLDSTSR	I		
									R	AIAELGIYPAVDPLDSTSR	I		
									R	IPSAVGYQPTLATDMGSM	I		
									R	IPSAVGYQPTLATDMGSM	I		
16	49	7.3	XP_564289.3	109	27.82	5.2	4(2)	16%	R	VENCDLFDGPK	S	Hexokinase	Carbohydrate metabolic process
									R	VENCDLFDGPK	S		
									K	AGLLFGGVGSDILFK	R		
									R	IGLIVGTGSNACYVER	V		
17	48	8.2	XP_314928.2	545	44.04	7.01	17(4)	30%	R	AAGLLLNK	E	Phosphoglycerate kinase	Carbohydrate metabolic process
									K	IVQNLVDK	A		
									R	IVAALDSIK	F		
									R	VDFNVPIK	E		
									R	VDFNVPIK	E		
									R	EAFAAPIAR	S		
									R	FYVEEEGK	G		
									K	LSIENVDLK	G		
18	48	8.7	XP_317672.2	514	46.88	6.43	22(6)	27%	K	YDLDFK	N	Enolase	Carbohydrate metabolic process
									K	KGVPLYK	H		

Table 3.1 (continued)

SN[a]	Exp. (MW[d]/pI[e])		NCBI accession NO.[b]	Protein score[c]	Theo. (MW[d]/pI[e])		Matching peptide	% coverage	Protein sequences			Recommended name	Biological process categories
18	48	8.7	XP_317672.2	514	46.88	6.43	22(6)	27%	K	ELDELMLK	L	Enolase	Carbohydrate metabolic process
									K	ACNCLLLK	V		
									K	ACNCLLLK	V		
									K	ACNCLLLK	V		
									K	ACNCLLLK	V		
									K	ACNCLLLK	V		
									K	ACNCLLLK	V		
									K	ELDELMLK	L		
									K	ELDELMLK	L		
									K	ELDELMLK	L		
									K	EALNLIQDAIAK	A		
									K	EALNLIQDAIAK	A		
									K	EALNLIQDAIAK	A		
									K	VEIGMDVAASEFHK	E		
									R	AAVPSGASTGVHEALELR	D		
									R	AAVPSGASTGVHEALELR	D		
									K	VNQIGSVTESINAHLLAK	K		
									K	VNQIGSVTESINAHLLAK	K		
									K	FGLDATAVGDEGGFAPNI	E		
									K	FGLDATAVGDEGGFAPNILENK	E		
19	45	6.2	ABD48797.2	378	42.00	5.3	9(6)	16%	R	AVFPSIVGR	A	Beta-actin	Cytoskeleton associated
									R	AVFPSIVGR	A		
									K	DSYVGDEAQSK	R		
									K	DSYVGDEAQSKR	G		
									K	IWHHTFYNELR	V		
									K	SYELPDGQVITIGNER	F		
									K	SYELPDGQVITIGNER	F		
									R	VAPEEHPVLLTEAPLNPK	A		
									R	VAPEEHPVLLTEAPLNPK	A		
20	45	6.5	AAY88916.1	282	42.07	5.3	7(2)	17%	R	DLTDYLMK	I	Actin	Cytoskeleton associated
									K	EITALAPSTIK	I		
									K	QEYDESGPSIVHR	K		

Table 3.1 (continued)

SN[a]	Exp. (MW[d]/pI[e])		NCBI accession NO.[b]	Protein score[c]	Theo. (MW[d]/pI[e])		Matching peptide	% coverage	Protein sequences			Recommended name	Biological process categories
									K	SYELPDGQVITIGNER	F		
									K	SYELPDGQVITIGNER	F		
									R	VAPEEHPVLLTEAPLNPK	A		
21	42	7.9	XP_319738.2	548	45.06	7.53	13(8)	22%	R	YILWR	I	Glutamine synthetase	Amino acid metabolism
									R	LETSSIDK	F		
									K	FSWGVADR	G		
									K	FSWGVADR	G		
									R	ALYKDPFK	A		
									K	CADDLWLSR	Y		
									K	CADDLWLSR	Y		
									R	ILEHSPNAHLNK	T		
									R	LETSSIDKFSWGVADR	G		
									K	YVQATYVWIDGTGENVR	L		
									K	YVQATYVWIDGTGENVR	L		
									K	AGPNDVIVLCDTYQPDGK	A		
									K	AGPNDVIVLCDTYQPDGK PTASNHR	A		
22	42	5.6	ABK88283.1	160	42.46	5.1	4(3)	7%	K	STVADNYR	R	Serpin	Amino acid metabolism
									K	QEVEVFLPK	F		
									K	SAFNAIATDSFR	S		
									K	SAFNAIATDSFR	S		
23	42	7.4	ADB80247.1	401	27.19	6.78	13(6)	39%	R	FWPTGR	G	Arginine kinase	Amino acid metabolism
									R	FLQAANACR	F		
									R	FLQAANACR	F		
									R	FLQAANACR	F		
									R	FLQAANACR	F		
									R	LVTAVNDIEK	R		
									R	LVTAVNDIEK	R		
									K	VSATLSGLEGELK	G		
									K	VSATLSGLEGELK	G		
									K	LEATADKYNLQVR	G		
									K	AVQQQLIDDHFLFK	E		
									R	GEHSEAEGGIYDISNK	R		

Table 3.1 (continued)

SN[a]	Exp. (MW[d]/pI[e])		NCBI accession NO.[b]	Protein score[c]	Theo. (MW[d]/pI[e])		Matching peptide	% coverage	Protein sequences			Recommended name	Biological process categories
24	40	8.8	XP_312372.4	320	39.99	8.49	8(3)	23%	R	ALQASVLR	A	Fructose-bisphosphate aldolase, class I	Carbohydrate metabolic process
									K	AAQEELIK	R		
									K	EIQEELAR	I		
									K	VTETVLAAVYK	A		
									K	GILAADESTATCGK	R		
									K	GILAADESTATCGK	R		
									K	KPTAQEIALATVTALR	R		
									R	IVPIVEPEILPDGDHDLER	C		
25	40	9.1	XP_312372.4	307	39.99	8.49	7(4)	16%	R	ALQASVLR	A	Fructose-bisphosphate aldolase, class I	Carbohydrate metabolic process
									R	ALQASVLR	A		
									K	AAQEELIK	R		
									K	VTETVLAAVYK	A		
									K	GILAADESTATCGK	R		
									K	GILAADESTATCGK	R		
									R	IVPIVEPEILPDGDHDLER	C		
26	39	9.5	XP_312372.4	504	39.99	8.49	10(8)	28%	R	ALQASVLR	A	Fructose-bisphosphate aldolase, class I	Carbohydrate metabolic process
									K	EIQEELAR	I		
									K	VTETVLAAVYK	A		
									K	VTETVLAAVYK	A		
									K	GILAADESTATCGK	R		
									K	KPTAQEIALATVTALR	R		
									K	KPTAQEIALATVTALR	R		
									R	IVPIVEPEILPDGDHDLER	C		
									R	IVPIVEPEILPDGDHDLER	C		
									R	IVPIVEPEILPDGDHDLER	C		
27	37	5.5	XP_003435947.1	350	32.50	4.79	8(3)	27%	K	IMELEEELK	V	Tropomyosin 1	Cytoskeleton associated
									K	IMELEEELK	V		
									K	SLEVSEDKANQR	V		
									K	LLTSTEANVAALTR	K		
									K	LLTSTEANVAALTR	K		
									K	LLEATQSADENNR	M		
									K	DNAQDKADTCENQAK	E		

Table 3.1 (continued)

SN[a]	Exp. (MW[d]/pI[e])		NCBI accession NO.[b]	Protein score[c]	Theo. (MW[d]/pI[e])		Matching peptide	% coverage	Protein sequences			Recommended name	Biological process categories
28	37	7.4	XP_308086.3	179	35.85	5.63	5(0)	10%	K	IDEGVVKR	E	Aldehyde reductase	ATP biosynthetic process
									R	EDLFITSK	L		
									K	REDLFITSK	L		
									K	AKIDEGVVKR	E		
									K	LWNTFHRPDLVEGACR	T		
29	37	7.8	XP_308082.4	115	36.80	5.95	4(0)	4%	K	LIEFCR	Q	Proton donor	ATP biosynthetic process
									R	EDVFIVTK	V		
									R	EDVFIVTK	V		
									K	REDVFIVTK	V		
30	34	8	XP_001648454.1	133	37.34	5.51	4(1)	9%	K	TSGQVILR	Y	Aldo-keto reductase	Unknown biological process
									R	QNIDIFDFK	L		
									R	QNIDIFDFK	L		
									K	LQFSDVDYIDTWK	A		
31	40	8	XP_313338.3	206	39.16	6.63	8(5)	10%	R	IGDFIVK	K	L-iditol 2-dehydrogenase	Unknown biological process
									R	VAIEPGYGCR	T		
									R	VAIEPGYGCR	T		
									K	VLVTDLLQNR	L		
									K	VLVTDLLQNR	L		
									K	VLVTDLLQNR	L		
									K	VLVTDLLQNR	L		
									R	LEQRPIPVPK	D		
32	39	7.99	XP_308279.2	157	38.62	6.27	6(2)	12%	R	GLGTQLLGK	I	Glycerol-3-phosphate dehydrogenase (NAD+)	Carbohydrate metabolic process
									K	FCETTIGCR	D		
									K	FVDVFYPGSK	L		
									K	FVDVFYPGSK	L		
33	38	8.8	XP_003436225.1	491	45.80	8.73	11(8)	24%	R	SLNLALR	K	Isocitrate dehydrogenase (NAD+)	Carbohydrate metabolic process
									R	MSDGLFLR	C		
									K	LITEEASNR	V		
									K	IQSACFETIK	E		
									K	FGIPQGAIDSVNR	N		
									K	FGIPQGAIDSVNR	N		
									K	CSEYTNAICDR	I		

Table 3.1 (continued)

SN[a]	Exp. (MW[d]/pI[e])		NCBI accession NO.[b]	Protein score[c]	Theo. (MW[d]/pI[e])		Matching peptide	% coverage	Protein sequences			Recommended name	Biological process categories
									K	TLYDNVDVVTIR	E		
									K	TLYDNVDVVTIR	E		
									K	EFNLYANVRPCR	S		
									R	KVTLIPGDGIGPEISAAVQK	I		
34	39	9.02	XP_001689093.1	175	45.87	8.64	7(2)	11%	R	MEELVMR	I	Coproporphyrinogen III oxidase	Porphyrin-containing compound biosynthetic process
									K	YFFIPHR	N		
									K	YFFIPHR	N		
									K	FGLYTPGAR	Y		
									K	FGLYTPGAR	Y		
									R	YVEFNLIYDR	G		
									K	AGVNISVVHGNLPK	G		
35	36	8.1											
36	34	8	XP_318487.4	359	34.68	8.66	11(3)	25%	K	APEGDFASK	T	Mitochondrial electron transfer flavoprotein subunit alpha	Lipid metabolism
									K	VGPVSEAAAK	L		
									K	SDRPSLTAAK	I		
									K	LGGDVTVLVAGTK	V		
									R	TIYAGNAIQTVK	S		
									K	TTEFVSQELTK	S		
									K	TTEFVSQELTK	S		
									K	TTEFVSQELTK	S		
									K	KLGGDVTVLVAGTK	V		
									R	AAVDAGYVPNDLQIGQTGK	I		
									R	AAVDAGYVPNDLQIGQTGK	I		
37	33	8.8	XP_316431.3	79	31.388	6.51	1(1)	3%	R	TSSGEALYIGR	A	Cytosol aminopeptidase	Amino metabolism
38	34	9.1	XP_319347.2	234	35.52	7.63	8(3)	14%	K	IWDLASK	T	Guanine nucleotide-binding protein subunit beta-2-like 1 protein	Signal transduction
39													
40													

Table 3.1 (continued)

SN[a]	Exp. (MW[d]/pI[e])		NCBI accession NO.[b]	Protein score[c]	Theo. (MW[d]/pI[e])		Matching peptide	% coverage	Protein sequences			Recommended name	Biological process categories
41	32	7.5	XP_312551.1	232	25.86	6.78	9(4)	19%	K	AEEEFNIEK	G	V-type H+-transporting ATPase subunit E	ATP biosynthetic process
									K	AEEEFNIEK	G		
									K	AEEEFNIEK	G		
									R	LKIMEYYEK	K		
									K	IQSSNMLNQAR	L		
									K	IQSSNMLNQAR	L		
									K	KIQSSNMLNQAR	L		
									R	LELIAQQLVPEIR	N		
									R	LELIAQQLVPEIR	N		
42	29	6.4	XP_308018.4	97	26.68	6.08	3(0)	14%	K	NLGIGVGETTK	D	NADH dehydrogenase (ubiquinone) flavoprotein 2	ATP biosynthetic process
									K	VADILGLPHMR	V		
									R	GAMIPLLDLAQR	Q		
43	29	8	XP_321710.2	567	28.75	6.34	24(15)	38%	K	AIESVANQGK	A	2,3-bisphosphoglycerate-dependent phosphoglycerate mutase	Carbohydrate metabolic process
									K	AIESVANQGK	A		
									R	HYGGLTGLNK	S		
									K	FLGDEETVR	K		
									K	FLGDEETVR	K		
									R	AQVTLDSILK	E		
									R	AQVTLDSILK	E		
									R	AQVTLDSILK	E		
									R	AQVTLDSILK	E		
									R	AQVTLDSILK	E		
									R	AQVTLDSILK	E		
									K	FDIAHTSLLTR	A		
									K	FDIAHTSLLTR	A		
									K	YGEEQVLIWR	R		
									K	YGEEQVLIWR	R		
									K	YGEEQVLIWR	R		
									K	YGEEQVLIWR	R		
									K	YGEEQVLIWR	R		
									R	TLPYWNDVIIPQLK	E		
									R	TLPYWNDVIIPQLK	E		

Table 3.1 (continued)

SN[a]	Exp. (MW[d]/pI[e])		NCBI accession NO.[b]	Protein score[c]	Theo. (MW[d]/pI[e])		Matching peptide	% coverage	Protein sequences			Recommended name	Biological process categories
									R	SFDVPPPNMEPDHAYYDA IVKDER	Y		
									R	SFDVPPPNMEPDHAYYDA IVKDER	Y		
									R	SFDVPPPNMEPDHAYYDA IVKDER	Y		
44	28	6.9											
45	26	5.5	XP_321467.4	451	26.73	6	14(6)	31%	K	ASITELCK	T	Triosephosphate isomerase	Carbohydrate metabolic process
									K	FCVGGNWK	M		
									K	FCVGGNWK	M		
									K	FCVGGNWK	M		
									K	FCVGGNWK	M		
									R	EAGQTEAVCFR	Q		
									K	GAFTGEISPAMLK	D		
									K	GAFTGEISPAMLK	D		
									K	VIACIGETLQER	E		
									K	VIACIGETLQER	E		
									R	AIFGETDELIAEK	V		
									R	AIFGETDELIAEK	V		
									R	AIFGETDELIAEK	V		
									K	DLGLGWVILGHSER	R		
46	27	7.98	XP_321467.4	598	26.73	6	21(9)	48%	K	ASITELCK	T	Triosephosphate isomerase	Carbohydrate metabolic process
									K	ASITELCK	T		
									K	FCVGGNWK	M		
									K	FCVGGNWK	M		
									K	FCVGGNWK	M		
									K	VAHALAEGLK	V		
									R	EAGQTEAVCFR	Q		
									R	EAGQTEAVCFR	Q		
									K	GAFTGEISPAMLK	D		
									K	GAFTGEISPAMLK	D		
									K	VIACIGETLQER	E		
									K	VIACIGETLQER	E		
									K	VIACIGETLQER	E		

Table 3.1 (continued)

SN[a]	Exp. (MW[d]/pI[e])		NCBI accession NO.[b]	Protein score[c]	Theo. (MW[d]/pI[e])		Matching peptide	% coverage	Protein sequences			Recommended name	Biological process categories
									R	IQYGGSVTAANCR	E		
									R	IQYGGSVTAANCR	E		
									R	AIFGETDELIAEK	V		
									R	AIFGETDELIAEK	V		
									K	DLGLGWVILGHSER	R		
									K	DLGLGWVILGHSER	R		
									R	RAIFGETDELIAEK	V		
									K	TATPEQAQEVHAALRK	W		
47	28	8.2	XP_319708.4	76	28.34	8.77	2(1)	6%	K	LADIPEGK	S	Cytochrome b-c1 complex subunit Rieske	ATP biosynthetic process
									R	VPDFSDYR	R		
48	25	6.2	XP_001662440.1	32	34.11	6.6	1(0)	2%	K	VISFDEVVK	T	Galactokinase	Carbohydrate metabolic process
49	26	6.7	XP_003436015.1	85	26.126	5.97	2(0)	15%	R	EIGHWLVGNIPGTK	V		
50	26	9.2	XP_001659009.1	194	27.45	7.6	5(2)	13%	K	AALDQFTR	C	Short-chain dehydrogenease/reductase	Unknown biological process
									K	LDVLVNNAGK	G		
									K	LDVLVNNAGK	G		
									K	VVIITGASSGIGAATAK	Y		
									K	VVIITGASSGIGAATAK	Y		
51	24	9.3											
52	23	9.2	AAR90328.1	62	23.18	8.24	5(0)	8%	K	IIQLGNAIK	F	superoxide dismutase 1	Response to oxidative stress
									K	IIQLGNAIK	F		
									K	IIQLGNAIK	F		
									R	SDPSAELQK	A		
									R	SDPSAELQK	A		
53	23	4.9	XP_317657.4	68	17.95	5.46	1(1)	5%	K	VFYDSANIR	Q	Short-chain dehydrogenease/reductase	Unknown biological process
54	19	5.4	XP_001660081.1	109	18.66	4.95	2(1)	11%	R	EAYEDVR	S	Conserved hypothetical protein	Unknown biological process
									K	AGGANYGTGVR	E		
55	20	6	XP_564212.2	205	17.96	5.19	5(3)	34%	K	SCGEETVIAIK	N	Eukaryotic translation initiation factor 5A	Translational elongation
									K	SCGEETVIAIK	N		

Table 3.1 (continued)

SN[a]	Exp. (MW[d]/pI[e])		NCBI accession NO.[b]	Protein score[c]	Theo. (MW[d]/pI[e])		Matching peptide	% coverage	Protein sequences	Recommended name	Biological process categories
56	22	7.8	XP_321834.4	123	20.86	8.3	5(1)	11%	K SGFAAEAQR K R QFSDEQLR A R QFSDEQLR A K GATQSGINFGNTR H K GATQSGINFGNTR H	Muscular protein 20	Unknown biological process
57	22	8.8	XP_308669.2	272	21.80	8.69	8(4)	24%	R FADENFK L K QTSWLDGR H K QTSWLDGR H R IVIGLFGGTVPK T R DFMIQGGDFTK G K DTNGSQFFITVK Q K DTNGSQFFITVK Q K DTNGSQFFITVK Q	Peptidyl-prolyl cis-trans isomerase	Protein folding
58	18	7.7	XP_320237.3	86	20.44	8.67	3(1)	13%	K GATQAGQNIGAGR K K GATQAGQNIGAGR K K FPAGVLYEDALR D	Muscular protein 20	Unknown biological process
59	18	8	ETN66360.1	417	24.88	8.09	8(5)	30%	R YVIFYIR D R YVIFYIR D K QIDVEVIGDR N K QIDVEVIGDR N K QIDVEVIGDR N K MLYSSSFDALK K K MLYSSSFDALK K K YIQATDLSEASR E K YIQATDLSEASR E K MLYSSSFDALKK S	Twinstar	Unknown biological process
60	16	6.3	XP_309573.2	210	15.34	5.57	5(2)	34%	K LGEWSGLCK I K LGEWSGLCK I K ICGASCVVLK D K DFGEETPALDVIK E K LITALCNEHQIPLIR V	40S ribosomal protein S12	Translationl elongation

Table 3.1 (continued)

SN[a]	Exp. (MW[d]/pI[e])		NCBI accession NO.[b]	Protein score[c]	Theo. (MW[d]/pI[e])		Matching peptide	% coverage	Protein sequences			Recommended name	Biological process categories
61	16	9	XP_003436444.1	451	14.85	7.68	11(8)	51%	K	SEGFDDYMK	A	Probable fatty acid-binding protein	Unknown biological process
									K	SEGFDDYMK	A		
									K	LGNSISPTVELVK	N		
									K	LGNSISPTVELVK	N		
									K	LGEEFDEETVDGR	M		
									K	LGEEFDEETVDGR	M		
									K	NGDEYTFNTLSTFK	N		
									K	NGDEYTFNTLSTFK	N		
									R	EFTATDLTATMTAGNAK	C		
									R	EFTATDLTATMTAGNAK	C		
									K	FKLGEEFDEETVDGR	M		
62	14	6.2	XP_553744.3	235	13.84	5.63	8(5)	29%	R	YIYLSGTDR	V	Profilin	Cytoskeleton associated
									R	YIYLSGTDR	V		
									R	YIYLSGTDR	V		
									R	YIYLSGTDR	V		
									R	YIYLSGTDR	V		
									K	SEGFEVSKEEVAK	I		
									K	SEGFEVSKEEVAK	I		
63	10	5.6	XP_001647949.1	106	9.51	6.7	3(3)	22%	K	VYAICGEIR	R	Hypothetical protein	Unknown biological process
									K	VYAICGEIR	R		
									R	MGESDDCIVR	L		
64	7	9.1	AAEL00388-PA	54	17.25	7.93	3(0)	8%	K	EGIPPDQQR	L	Ubiquitin	Unknown biological process
									K	IEDKEGIPPDQQR	L		
									K	IEDKEGIPPDQQR	L		
65	16	8.3	XP_308641.4	326	18.68	6.75	9(6)	27%	K	EIALWFK	D	Nucleoside-diphosphate kinase	Nucleoside triphosphate biosynthetic process
									R	GDLCVQVGR	N		
									R	GDLCVQVGR	N		
									R	GDLCVQVGR	N		
									R	GDLCVQVGR	N		
									R	NIIHGSDAVESANK	E		
									R	NIIHGSDAVESANK	E		
									R	NIIHGSDAVESANK	E		

Table 3.1 (continued)

SN[a]	Exp. (MW[d]/pI[e])		NCBI accession NO.[b]	Protein score[c]	Theo. (MW[d]/pI[e])		Matching peptide	% coverage	Protein sequences			Recommended name	Biological process categories
									K	MLGATNPADSEPGTIR	G		
66	16	5.3	XP_309490.3	207	17.40	5.27	7(1)	31%	K	IIVSALK	A	Cytochrome c oxidase subunit Va precursor	ATP biosynthetic process
									K	IIVSALK	A		
									R	LNDYALAVR	F		
									R	LNDYALAVR	F		
									K	AMNDLLGMDLVPEPK	I		
									R	KAMNDLLGMDLVPEPK	I		
									R	YEAYFNRPEIDGWEAR	K		

[a]Spot number refers to those shown in Figure 3.4

[b]Accession number of the best hit of proteins from mosquitoes and/or arthropod species

[c]Mowse score ≥ 30

[d]MW: molecular mass

[e]pI: isoelectric point

3.2 Changes in the female salivary glands of *An. dissidens* during adult development and after blood feeding

3.2.1 Salivary gland morphology

By light microscopy, it showed that morphology of female salivary glands of *An. dissidens* mosquitoes aged seven days consisted of a distinctive tri-lobed structure connected to a main salivary canal, a single medial and two lateral lobes with proximal and distal secretory portions. The proximal portion of the median lobe was short and served to link this lobe with the two lateral lobes. A cuticular duct extended through it from the distal portion and connected to the ducts of the lateral lobes.

By TEM observation, the salivary glands of female mosquitoe aged between zero to 21 days were shown in Figure 3.5-3.8. Micrographs revealed that all lobes were acinar structures, organized as a unicellular epithelium that surrounded a salivary canal and surrounded by a very thin basal lamina. Cellular architecture was similar among the lobes, with secretory material appearing as large masses that pushed the cellular structures to the periphery of the organ. In the cytoplasm of all secretory cells, rough endoplasmic reticulum cisternae (RER) with several mitochondria (M) were observed. Nuclei were also basally located and exhibited a more or less prominent central nucleolus. In cells of the proximal-lateral lobes, secretory cavities contain secretory mass with finely filamentous aspect (Figure 3.5). Numerous short MV extended from the apical cell membrane into the cavities. The secretory cavities (Sc) opened into a periductal space (Ps) and the secretory product seemed to reach the duct lumen through irregular channels that perforate the cuticular wall of the proximal salivary duct (Figure 3.5). In the distal-lateral lobes, cells had Sc filled with a dense secretory product with a mottled pattern (Figure 3.6). A large number of mitochondria, rough endoplasmic reticulum, and free ribosomes were found in the cytoplasm of the cells. The secretory masses of the distal lateral portion appeared to open directly into the duct, whose cuticle is perforated by broad channels; the dark secretory product completely filled the duct lumen. The apical cell membrane forms a very intricate network that surrounds the Sc (Figure 3.6b). Cells of the medial lobe hold large Sc containing secretory masses uniformly stained and highly electron-dense (Figure 3.6). Short membrane projections protruding from the apical cell

membrane into the secretory cavities were observed. The cytoplasm of the cells contained abundant cisternae of rough endoplasmic reticulum and mitochondria with large nucleoli noted (Figure 3.7). Non-secretory cells of the proximal portion of the medial lobe were shown as Figure 3.8. Seven to eight cells make up the circumference of the proximal portion epithelium. The apical cell membranes are united by septate desmosomes. A high number of mitochondria and a large nucleus in the basal cytoplasm of each non-secretory cell were thrown into numerous deep membrane infoldings penetrating into onefourth to one-third of the depth of the cells. A very dense and ruffled cuticular wall with no channels limited the salivary duct, which had its lumen occupied by a very uniform and electron-dense secretory material (Figure 3.8a, b).

Following emergence, the glands of newly emerged females were poorly developed but their growth was progressive from the time of emergence. The glands accumulated secretory material rapidly and developed completely within three days post emergence. In all lobes, degenerative changes including loss of stored secretion and increase of cytoplasmic vacuolation and concentric lamellar structures were observed from 16 days post emergence. After blood feeding, the cellular architecture was also similar the salivary gland during adult development. However, saliva contents in all lobe were released through a salivary canal, but no completely released in each secretory cell. Saliva depletion was affected by reduced size of secretory cell and also wrinkled basal lamina.

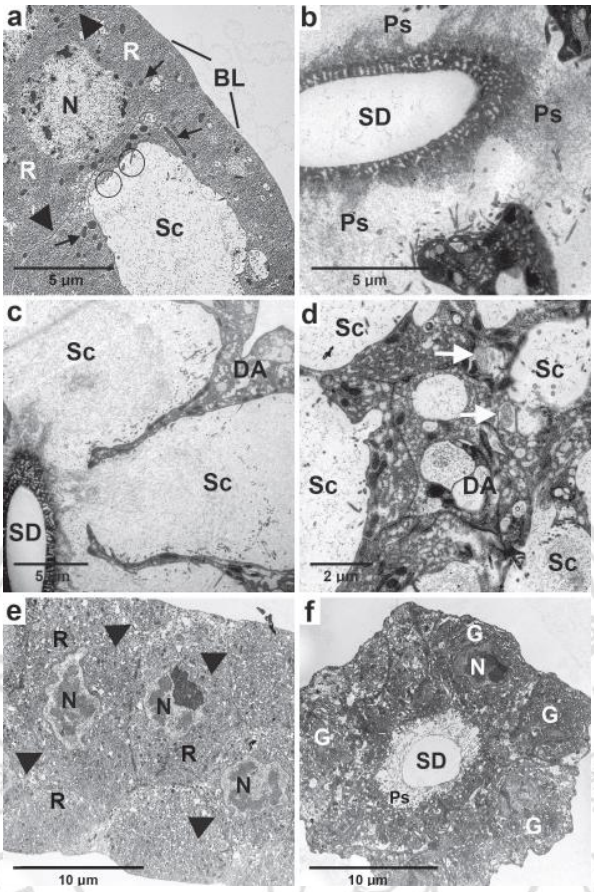

Figure 3.5 TEM micrographs of proximal-lateral lobes of adult female glands. a) A proximal-lateral lobe of an adult female gland of a newly emerged female. The epithelial cells contain rough endoplasmic reticulum (R), mitochondria (arrows) and nucleus (N) with masses of condensed chromatin. Short microvilli (circles) protrude into a secretory cavity (Sc). The secretory cavity is filled with finely granular secretion. A thin basal laminar (BL) encompasses the cell periphery. Arrowheads indicate septate desmosomes which unite the lateral cell membranes of the epithelial cells. b) The duct and periductal space (Ps) of the proximal-later portion. A filamentous meshwork surrounding the granular material similar to the secretion product filled the periductal space. c, d) The proximal-lateral lobes of mosquitoes aged 16 and 21 days post emergence, respectively, showing degenerative areas (DA) with cytoplasmic vacuoles and concentric lamellar structures (white arrows). e, f) The intermediate region between proximal-lateral and distal-lateral lobes. e) Cells surrounding the duct display numerous rough endoplasmic reticulum (R) from the basal region to the periductal space (PS). f) Higher magnification display a part of the salivary duct (SD). A part of a large nucleus (N) and the presence of large granules (G) associated with basal membrane invaginations were observed.

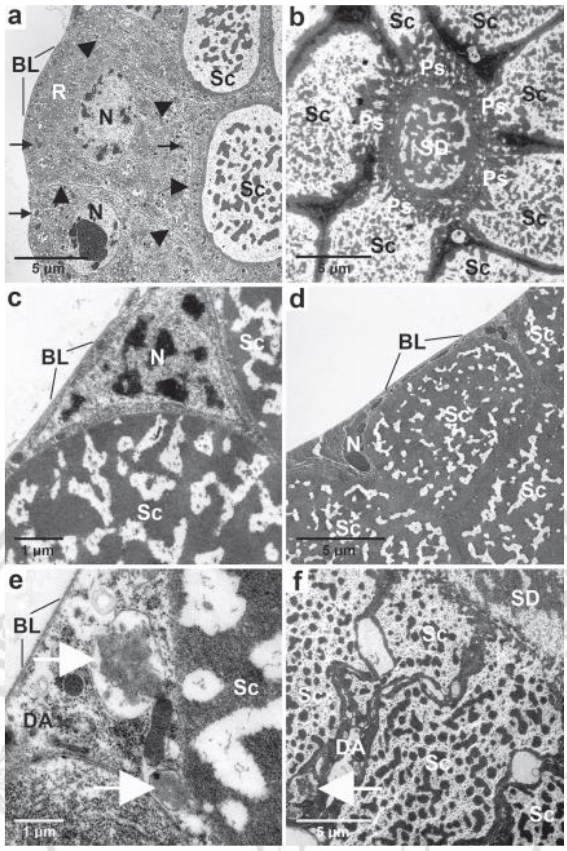

Figure 3.6 TEM micrographs of distal-lateral lobes of adult female glands. a) A newly emerged female. The epithelial cells contain rough endoplasmic reticulum (R), mitochondria (arrows) and nucleus (N). A nucleoli with large condensed chromatin masses was noted. Secretory cavities (Sc) were filled with coarsely granulated material. The secretory material has a mottled pattern. A thin basal laminar (BL) encompasses the cell periphery. Arrowheads indicate septate desmosomes of the epithelial cells. b) A salivary duct and periductal space (Ps) of the distal-later portion. The duct surrounds with at least seven epithelial cells. Each cell has a large secretory cavity. A filamentous meshwork and granular material similar to the secretion product fills the periductal space. c) An epithelial cell from a mosquito aged seven days post emergence showing a nucleus (N) with condensed chromatin masses, secretory cavities (Sc) filled with coarsely granulated material. and a thin basal laminar (BL). d) Epithelial cells from a mosquito aged 16 days post emergence showing a nucleus (N) with large condensed chromatin masses, secretory cavities (Sc), and a thin basal laminar (BL). e, f) Shrinking epithelial cells with loss of stored secretion and degenerative areas (DA) with vacuoles and concentric lamellar structures (white arrows) were observed in from the mosquitoes aged 21 days post emergence.

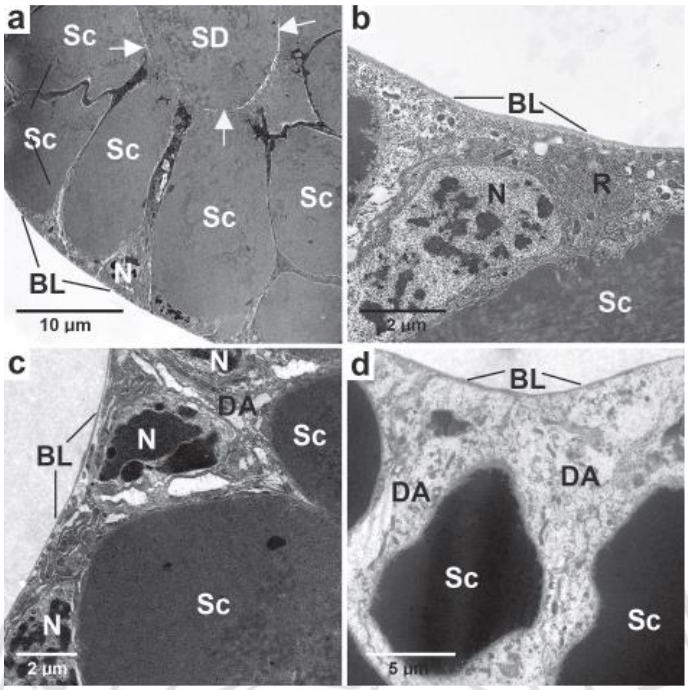

Figure 3.7 TEM micrographs of cells in the medial lobe of adult female glands. a) Epithelial cells from a mosquito aged three day post emergence. The epithelial cells contain nucleus (N) and secretory cavities (Sc) filled with dark homogeneous material. A thin basal laminar (BL) encompasses the cell periphery. b) Cells from a mosquito aged seven day post emergence showing a nucleus (N) with condensed chromatin masses, rough endoplasmic reticulum (R), secretory cavities (Sc) and a thin basal laminar (BL). c) Epithelial cells from a mosquito aged 16 days post emergence showing nucleus (N) with large condensed chromatin masses, secretory cavities (Sc), and a thin basal laminar (BL). Degenerative areas (DA) is noted. d) Shrinking epithelial cells with loss of stored secretion and degenerative areas (DA) with vacuoles and concentric lamellar structures (white arrows) were observed in cells from the mosquitoes aged 21 days post emergence.

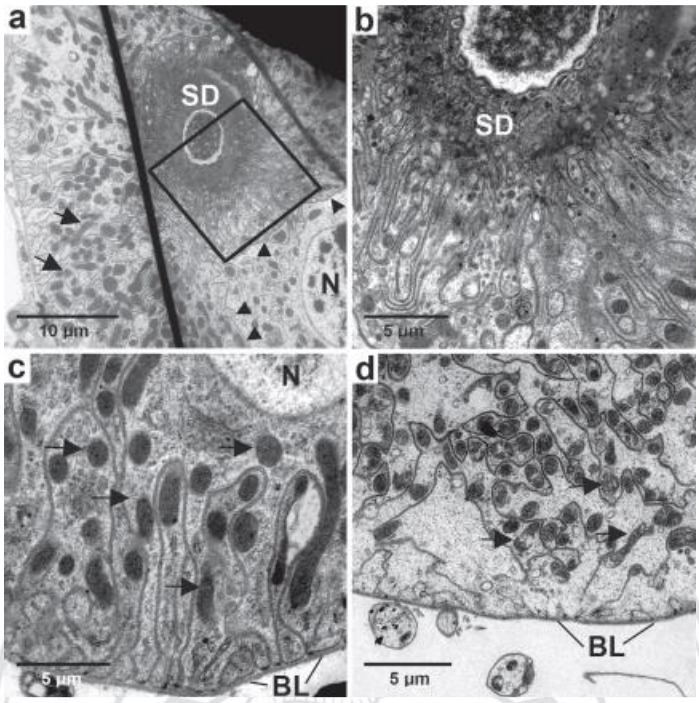

Figure 3.8 TEM micrographs of the proximal portion of the medial lobe. a) The salivary duct (SD) with a ruffled wall. Cells surrounding the duct display numerous and deep infoldings of membrane extended from the basal region to the periductal space. The infoldings contain a high number of mitochondria (arrows) and almost no cytoplasm. Arrowheads indicate septate desmosomes. b) Higher magnification of boxed region in (a) displaying a part of the salivary duct (SD) and infolded apical cell membranes. c) A part of a large nucleus (N) and the presence of numerous tubular mitochondria (arrows) associated with basal membrane invaginations were observed. d) At 21 days post emergence, degradation of mitochondria (arrows) and vesicles were observed. Basal laminar (BL).

3.2.2 Salivary gland proteins

Following age associated protein changes, SDS-PAGE analysis revealed at least 11 major protein bands in the female glands. In newly emerged females, protein bands of molecular masses higher than 32 kDa were weakly visualized. Then the number of protein components gradually increased with age (Figure 3.9). The different morphological regions of the female salivary glands displayed different electrophoretic protein profiles. The major protein bands with molecular masses of 65, 37, 34, 20, 18, and 10 kDa appeared predominantly in the distal portions of the lateral lobes (Figure 3.9, lane D), while protein bands with molecular masses of 45, 39, 35, 33, and 14 kDa were predominant in the medial lobe (Figure 3.9, lane M). As the proximal portions of the lateral lobes were very small, 50 proximal portions from 25 females were used to analyze on a SDS gel. The protein profile shows a number of minor protein bands (Figure 3.9, lane P).

The 2-DE of salivary gland samples collected 0, 1, 3, 12, 16 and 21 days after emergence are shown in Figure 3.10. The proteins accumulated following emergence, to reach a typical profile after 1 day (Figure 3.10b). The profile consisted of approximately 80 well-resolved spots with molecular masses of 13 to 80 kilodaltons and isoelectric points ranging from 3.8 to 10. Of these, there were 17 major salivary gland proteins observed from 1 to 21 days after emergence for which peptide sequence data was obtained (Table 3.2). These were each given a spot number (SN) from 1 to 17 (Table 3.2, Figure 3.10b). In newly emerged mosquitoes (day 0), the 2D profile revealed 9 of the 17 major protein spots, namely spot numbers SN3, 7-11, 13, 15 and 17 (Figure 3.10a). The remaining 8 major spots were first detected in the salivary glands of females on day 1 after emergence. Each of the 17 major protein spots were excised and subjected to nanoLC-MS for identification. The results of mass spectrometry analysis are summarized in Table 3.2. The 17 major protein spots gave significant matches to protein sequences from various species of mosquito. The identified proteins included three apyrases (SN 1-3), four putative-mucin like proteins (SN 4-7), an anti-platelet protein (SN 8), two long form D7 proteins (SN 9 and 10), a gVAG precursor (SN 11), three short form D7 related proteins (SN 12-14), two gSG7 proteins (SN 15 and 16) and gSG6 (SN 17).

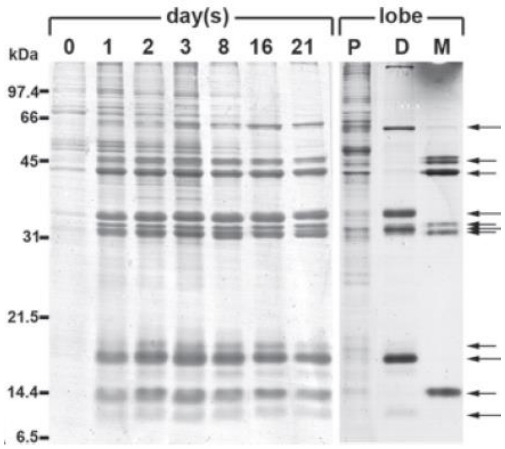

Figure 3.9 SDS-PAGE protein profiles of salivary glands of female *An. dissidens* mosquitoes. Proteins of each female salivary gland pair from a mosquito ages varying from 0 to 21 days separated in a 15% SDS polyacrylamide gel and CBB stained. Lane P: fifty proximal portions of the lateral lobes; lane D: two distal portions of the lateral lobes; lane M: two medial lobes. Molecular mass markers are indicated on the left in kDa. Numbers at the top indicate age in days post emergence. Arrows indicate major salivary gland proteins of female mosquitoes.

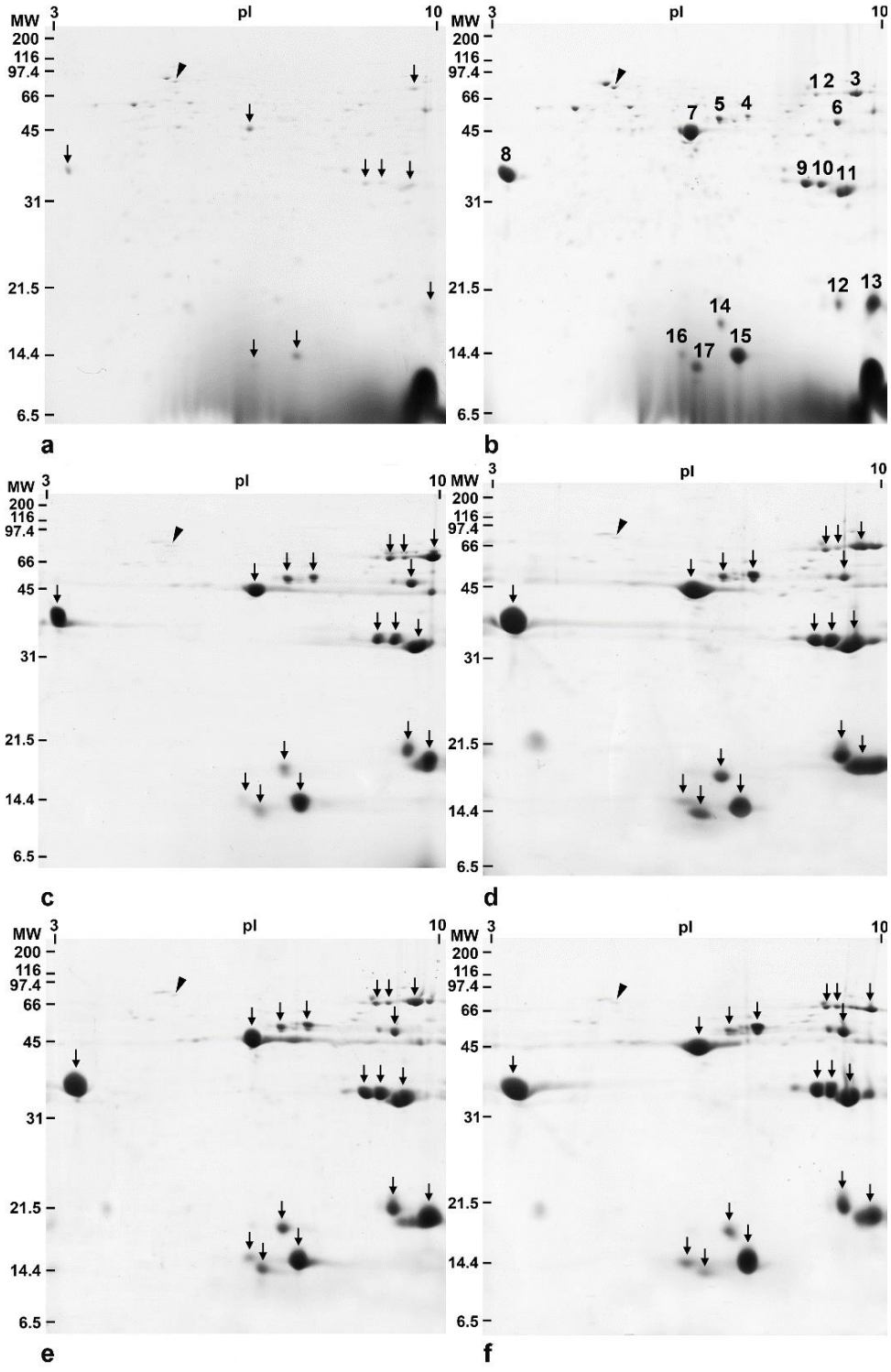

Figure 3.10 2-DE analysis of female salivary gland proteins of *An. dissidens* mosquitoes according to age. Molecular mass markers are indicated on the left in kDa. Isoelectric points (pI) are indicated at the top. Numbers indicate major salivary gland proteins. a: a representative of 2-D gels of proteins extracted from 80 female mosquitoes aged 0 day; b: 1 day; c: 3 days; d: 12 days; e: 16 days; f: 21 days.

Table 3.2 Details of 17 major protein spots identified by nano-liquid chromatography-mass spectrometry in the female salivary glands of *An. dissidens.*

SN[a]	Accession number[b], Protein description [species]	Protein score[c]	No. of peptides/ % coverage	Database Mw[d]/ pI[e]	Observed Mw/ pI	Peptide sequence(s)
1	CAB40345, apyrase [*Anopheles gambiae*]	65	1/1	62.08/ 8.88	68/ 8.8	R.VFHTVQELR.K
2	CAB40345, apyrase [*Anopheles gambiae*]	57	1/1	62.08/ 8.88	68/ 8.9	R.VFHTVQELR.K
3	AAO06829, salivary apyrase [*Anopheles stephensi*]	50	1/1	64.70/ 6.77	68/ 9.7	R.LTVYFDQR.G
4	AAL85611, putative mucin-like protein [*Aedes aegypti*]	35	1/3	28.96/ 5.10	56/ 7.6	M.AVTISHSK.V
5	AAL85611, putative mucin-like protein [*Aedes aegypti*]	35	1/3	28.96/ 5.10	55/ 7.2	M.AVTISHSK.V
6	AAL85611, putative mucin-like protein [*Aedes aegypti*]	35	1/3	28.96/ 5.10	54/ 9.3	M.AVTISHSK.V
7	AAL85611, putative mucin-like protein [*Aedes aegypti*]	35	1/3	28.96/ 5.10	48/ 6.8	M.AVTISHSK.V
8	KFB41046, anti-platelet protein [*Anopheles sinensis*]	212	4/18	26.78/ 4.12	38/ 4	R.LMNPTIDLVNTIEK.Y K.DVQGLVKESEK.S R.ELDEGLIDR.E R.EQELSDCIVDKR.D
9	KFB42863, long form D7 salivary protein [*Anopheles sinensis*]	180	5/15	35.63/ 8.35	35/ 8.7	K.VYAADPSIK.K K.KGESYFAYCEK.R R.QYELTGSAQLK.D K.DSIDCIFR.G R.SANYAYLVLGK.V
10	KFB42863, long form D7 salivary protein [*Anopheles sinensis*]	254	5/15	35.63/ 8.35	34/ 9	K.VYAADPSIK.K K.KGESYFAYCEK.R R.QYELTGSAQLK.D K.DSIDCIFR.G R.SANYAYLVLGK.V
11	KFB54026, putative gVAG protein precursor [*Anopheles sinensis*]	117	2/7	31.51/ 9.31	33/ 9.4	K.QFPYAGQNIAITK.Y K.VGCSLWYWK.D
12	AAL16039, short form D7r1 salivary protein [*Anopheles arabiensis*]	43	1/6	19.04/ 9.17	20/ 9.3	K.LIKPLNAIEK.D
13	ACR54288, a348 (D7 related) [*Anopheles anthropophagus*]	389	6/27	18.96/ 9.34	19/ 9.8	K.TIGFVDK.D K.TIGFVDKDGR.G K.LIKPLNAIEK.D K.CMLQSNSAESFK.K K.CMLQSNSAESFKK.V K.VFDLTELVLAGK.L
14	KFB42861, D7-related 3.2 protein [*Anopheles sinensis*]	142	2/5	18.68/8.12	18/ 7.2	K.KAVDYVELLR.A K.AVDYVELLR.A
15	KFB36874, gSG7 salivary protein [*Anopheles sinensis*]	130	2/8	16.79/5.94	16/ 7.3	K.YGVQVQLR.E K.YGVQVQLREPLVK.K

Table 3.2 (continued)

SN[a]	Accession number[b], Protein description [species]	Protein score[c]	No. of peptides/ % coverage	Database Mw[d]/ pI[e]	Observed Mw/ pI	Peptide sequence(s)
16	KFB36874, gSG7 salivary protein [*Anopheles sinensis*]	68	1/5	16.79/5.94	14/ 6.6	K.YGVQVQLR.E
17	CAC35522, gSG6 protein [*Anopheles gambiae*]	50	1/8	13.66/ 5.3	12 / 6.8	K.QKQWIDR.D
Control	ABF18332, heat shock cognate 70 [*Aedes aegypti*]	316	7/11	71.4/5.3	77.0/5.4	R.TTPSYVAFTDTER.L K.NQVAMNPTNTIFDAK.R K.DAGTISGLNVLR.I R.IINEPTAAAIAYGLDK.K R.IINEPTAAAIAYGLDKK.T K.LLQDFFNGK.E K.FELSGIPPAPR.G

[a]Spot number refers to those shown in Figure 3.10b

[b]Accession number of the best hit of proteins from mosquitoes and/or arthropod species

[c]Mowse score ≥ 30

[d]MW: molecular mass

[e]pI: isoelectric point

The relative expression levels of the 17 major protein spots determined at different ages in adult development are shown in Figure 3.11 and Appendix A. The 17 protein spots varied in their expression across the 8 time points sampled (0, 1, 2, 3, 8, 12, 16 and 21 days). Although there was variation observed, the patterns of expression could be placed into four groups. The largest (Group 1) was represented by SN4, 10, 11, 13, 15 and 16, which tended to show a more or less steady increase in expression with age of mosquito, but reaching a plateau at the latter time points. Another large group (Group 2) consisted of SN1, 2, 5, 7, 9 and probably SN3, in which the relative expression climbed rapidly to day 3, and then remained more or less constant for the remaining time points, except SN3 that dropped off at the last time point. The third group (Group 3) included SN8, 12, 14 and 17, which showed an early steep rise, a levelling off, then a peak on day 12, and decreased expression thereafter. Finally, there was SN6 (Group 4), which showed a unique expression pattern, rising to peak at day 3, and then steadily falling thereafter. A homologue of a heat shock cognate 70 kDa protein from *Ae. aegypti* (accession number ABF18332) was used as an internal control in the 2-DE gels. This control protein is indicated by an arrowhead in each panel of Figure 3.10 and showed no significant difference in density between samples.

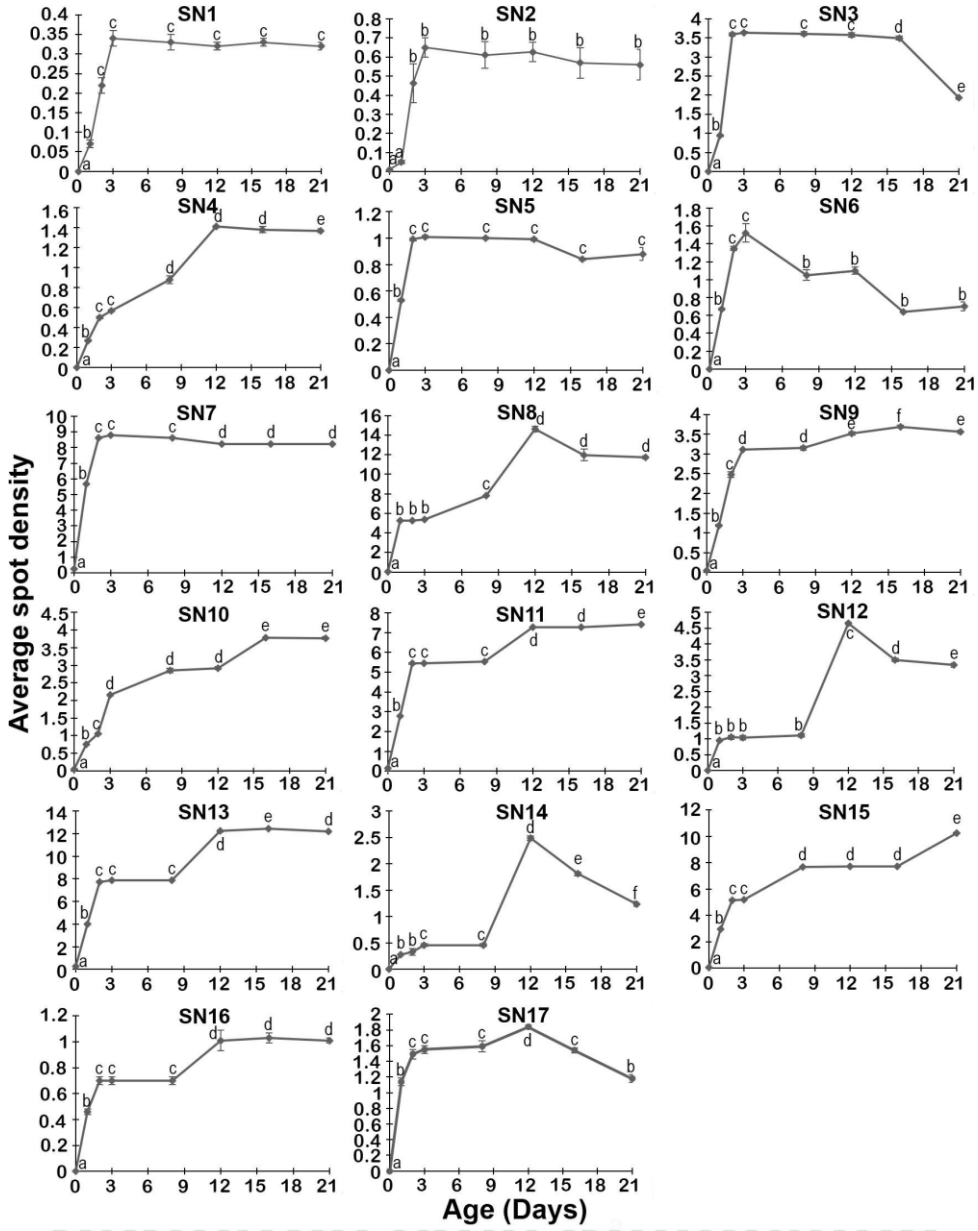

Figure 3.11 Expression volumes of the 17 major protein spots in the female salivary gland of *An. dissidens* at different times post emergence. The y-axis represents relative expression level normalized with heat shock cognate (HSC) 70, and the x-axis represents different ages on days 0, 1, 2, 3, 8, 12, 16, and 21, accordingly. Different letters (a, b, c, d, e, f) indicate significantly different levels of protein expression ($p < 0.05$), i.e. groups labelled with one letter (e.g. "a") are not significantly different from each other, but are different to groups labelled with a different letter (e.g. b, c, d, e, or f), and so on. Any given letter is only relevant within that protein (i.e. "a" in SN1 has nothing to do with "a" in SN2). Error bars are plotted for all points, but are too small to be visualized in some cases.

Salivary gland proteins of sugar-fed and blood-fed female *An. dissidens* were analyzed using 2-DE (Figure 3.12). The amount of depletion of each major salivary gland protein as a result of blood feeding was determined by comparison between the two groups (Table 3.3). Fifteen out of the 17 protein spots showed significant depletion after blood feeding, the exceptions being SN2 and SN12. The amount of depletion in the 15 spots varied from 8.5% for SN6 up to 68.11% for SN5, with a range of values in between for the other 13 spots.

Table 3.3 Amounts of depletion of the major salivary gland proteins after blood feeding of *An. dissidens* mosquitoes.

SN[a]	ASD ± SD[b]		Amount depleted	% depletion
	Sugar fed	Blood fed		
1	0.45 ± 0.02	0.34 ± 0.02	0.11 ± 0.04	25.41[c]
2	0.90 ± 0.03	0.88 ± 0.02	0.02 ± 0.04	1.86
3	4.55 ± 0.01	3.02 ± 0.01	1.53 ± 0.01	33.65[c]
4	0.98 ± 0.02	0.55 ± 0.02	0.42 ± 0.03	43.29[c]
5	1.63 ± 0.03	0.52 ± 0.03	1.11 ± 0.00	68.11[c]
6	1.11 ± 0.02	1.01 ± 0.03	0.09 ± 0.04	8.15[c]
7	10.86 ± 0.02	5.52 ± 0.02	5.35 ± 0.02	49.21[c]
8	11.23 ± 0.02	5.86 ± 0.02	5.37 ± 0.01	47.82[c]
9	4.01 ± 0.04	2.30 ± 0.03	1.71 ±0.02	42.57[c]
10	3.60 ± 0.03	1.92 ± 0.02	1.68 ± 0.04	46.63[c]
11	7.94 ± 0.02	5.31 ± 0.03	2.62 ± 0.02	33.07[c]
12	3.06 ± 0.02	3.02 ± 0.02	0.04 ± 0.04	1.25
13	12.55 ± 0.03	9.67 ± 0.03	2.88 ± 0.02	22.92[c]
14	2.08 ± 0.02	1.08 ± 0.02	1.00 ± 0.02	48.15[c]
15	6.71 ± 0.02	4.12 ± 0.02	2.59 ± 0.03	38.58[c]
16	0.98 ± 0.01	0.56 ± 0.02	0.41 ± 0.01	42.49[c]
17	2.01 ± 0.03	0.95 ± 0.01	1.07 ± 0.04	52.99[c]

[a]Spot number refers to those shown in Figure 3.10b

[b]ASD ± SD = Average spot density ± Standard deviation

[c]Student's *t*-test, $p < 0.05$

3.3 Bacterial diversity of female *An. dissidens* midguts

Midgut bacterial microflora (MF) of the sugar fed female *An. dissidens* (5 days old) were characterized by culture-dependent (on LB agar) and culture-independent (direct amplification of 16S rRNA gene) methods. Species of the MF were identified based on 16S rRNA sequences.

3.3.1 Analysis of cultivable bacteria from the midgut of female *An. dissidens*

Pools of five the mosquito midguts were homogenized in 1X PBS and plated on LB agar for isolation of the cultivable microflora. Morphology of bacterial colonies was studied based on the colony size, shape, color and margin. Sixteen colonies were selected and identified based on 16S rRNA gene sequence. A BLASTn search result of each sequence with more than 97% similarity was considered to be of the same operational taxonomic units (OTUs). In this study, approximately 80% of the mosquitoes contained cultivable MF in the midguts. An average number of MF was 86 CFU/ml. Most of the identified bacteria belonged to the family of Enterobacteriaceae (43%), Pseudomonadaceae (12.5%), Thorselliaceae (12.5%), Enterococcaceae (12.5%), and so on. Details of MF community composition and relative abundance at level of each genus are shown in Table 3.4.

3.3.2 Analysis of uncultivable MF from the midgut of female *An. dissidens*

A 16S rRNA gene library was constructed from pools of five female *An. dissidens* midguts. Sixty white colonies from the liberary were randomly selected for 16S rRNA PCR amplification. Only 14 from 60 colonies were successfully amplified, and the PCR products (approximately 1,500 bp) were sent sequencing. The results were showed that the predominant bacteria belonged to the genus *Thorsellia* (71%), *Asaia* (21%), and *Thermoactinomyces* (14%) (Table 3.4).

Table 3.4 Lists of cultivable and uncultivable bacteria from the midgut of laboratory-reared *An. dissidens* base on 16S rRNA sequencing.

Method	Clone number	GenBank accession number	Closest relative according to Blast (%identity)
Using culture independence method	A1mb5d001	NR_113845.1	*Asaia siamensis* strain NBRC 16457 (99%)
	A1mb5d002	NR_118583.1	*Thermoactinomyces daqus* (99%)
	A1mb5d003	NR_043217	*Thorsellia anophelis* strain H2.1 (98%)
	A1mb5d004	NR_112953.1	*Asaia spathodeae* strain GB23-2 (99%)
	A1mb5d005	FJ608080.1	Uncultured *Thorsellia* sp. clone LC47 (98%)
	A1mb5d006	KF921010.1	*Thermoactinomyces daqus* (99%)
	A1mb5d015	NR_043217.1	*Thorsellia anophelis* strain H2.1 (98%)
	A1mb5d047	NR_043217.1	*Thorsellia anophelis* strain H2.1 (97%)
	A1mb5d051	NR_043217.1	*Thorsellia anophelis* strain H2.1 (97%)
	A1mb5d055	EF434777.1	Uncultured *Thorsellia sp*. clone 895T7W2 (99%)
	A1mb5d057	NR_113845.1	*Asaia siamensis* gene (99%)
	A1mb5d060	NR_043217.1	*Thorsellia anophelis* strain H2.1 (98%)
	A1mb5d066	NR_043217.1	*Thorsellia anophelis* strain H2.1 (98%)
	A1mb5d085	FJ608066.1	Uncultured *Thorsellia* sp. clone LC32 (99%)
Using culture dependent method	BP3.1	JN257136.1	*Pseudomonas fulva* (99%)
	BS2.2	KJ184887.1	*Enterobacter* sp. (99%)
	BS2.3	AB904773	*Enterococcus gallinarum* (99%)
	BS2.4	KJ184887	*Enterobacter* sp. (99%)
	BS2.5	KJ184850	*Enterobacter* sp. (99%)
	BS4.3	AB571232	*Agrobacterium tumefaciens* (99%)
	NV2.2.1	AB641895	*Pantoea* sp. (99%)
	BS2.1	AB904773	*Enterococcus gallinarum* (99%)
	BS2.2	JQ659623	*Enterobacter asburiae* strain R2-343 (99%)
	NV2.1	AB641895.1	*Pantoea* sp. (97%)
	BV4.1	KF285965.1	*Pseudomonas oryzihabitans* strain 8t4 (95%)
	BV4.2	FJ608128.1	*Thorsellia anophelis* strain L34 (99%)
	Nv3.1	NR_043217.1	*Thorsellia anophelis* strain H2.1 (97%)
	5LAb1	EU293342.1	*Comamonas* sp. (98%)
	5LAb2	KC430995.1	*Bacillus* sp. (97%)
	5LAb3	CP009863.1	*Klebsiella pneumoniae* (98%)